

On the trigger mechanisms for SGR giant flares

Ramandeep Gill* and Jeremy S. Heyl†

*Department of Physics and Astronomy, University of British Columbia, 6224 Agricultural Road,
Vancouver, British Columbia, Canada V6T 1Z1*

Accepted —. Received —; in original form —

ABSTRACT

We examine two trigger mechanisms, one internal and the other external to the neutron star, that give rise to the intense soft gamma-ray repeater (SGR) giant flares. So far, three giant flares have been observed from the three out of the seven confirmed SGRs on March 5, 1979, August 27, 1998, and December 27, 2004. The last two events were found to be much more powerful than the first, and both showcased the existence of a precursor, that we show to have had initiated the main flare. In the internal mechanism, we propose that the strongly wound up poloidal magnetic field develops tangential discontinuities and dissipates its torsional energy in heating the crust. The timescale for the instability to develop coincides with the duration of the quiescent state that followed the precursor. Alternatively, we develop a reconnection model based on the hypothesis that shearing motion of the footpoints causes the materialization of a Sweet-Parker current layer in the magnetosphere. The thinning of this macroscopic layer due to the development of an embedded super-hot turbulent current layer switches on the impulsive Hall reconnection, which powers the giant flare. Again, we show that the thinning time is on the order of the preflare quiescent time. This model naturally explains the origin of the observed nonthermal radiation during the flares, as well as the post flare radio afterglows.

Key words: stars: magnetic fields - stars: neutron - magnetars

1 INTRODUCTION

The soft gamma-ray repeaters (SGRs) showcase flux variability on many different timescales. The quiescent state, with persistent X-ray emission ($L_X \sim 10^{35}$ erg s $^{-1}$), punctuated by numerous sporadic short bursts of gamma-rays, with peak luminosities up to $\sim 10^{42}$ erg s $^{-1}$ and typical duration in the range $\sim 0.01 - 1$ s, mark the defining characteristics of SGRs (see Mereghetti 2008 and Woods & Thompson 2006 for a review). Out of the seven confirmed SGR sources, SGR 0525-66, SGR 1806-20, SGR 1900+14, SGR 1627-41, SGR 1150-5418, SGR 0418+5729, SGR 0501+4516 (with the last three added recently to the SGR family; see Kaneko et al. 2010; van der Horst et al. 2010; Kumar et al. 2010), the first three have been known to emit giant flares. A rare phenomenon compared to the commonly occurring short bursts, the giant flares unleash a stupendous amount of energy ($\sim 10^{44}$ erg) in gamma-rays over a timescale of $\sim 0.2 - 0.5$ s in a fast rising initial peak. The initial high energy burst is followed by a long ($\sim 200 - 400$ s), exponentially decaying pulsating tail of hard X-ray emission, the period of which coincides with that of the rotation

of the neutron star (NS). Additionally, intermediate strength but rare outbursts lasting for few tens of seconds have been observed in the case of SGR 1900+14.

The first extremely energetic giant flare from a recurrent gamma-ray source, SGR 0525-66, was detected on March 5, 1979 by the gamma-ray burst detector aboard the Venera 11 & 12 space probes and the nine interplanetary spacecraft of the burst sensor network (Mazets et al. 1979; Helfand & Long 1979). The position of the source was found to be coincident with the supernova remnant N49 at a distance of ~ 55 kpc in the Large Magellanic Cloud. The flare consisted of a sharp rise (~ 15 ms) to the peak gamma-ray luminosity, $L_\gamma \sim 10^{44}$ erg s $^{-1}$, subsequently followed by an exponentially decaying tail with $L_\gamma \sim 10^{42}$ erg s $^{-1}$. Remarkably, the initial burst only lasted for ~ 0.1 s compared to the longer lasting (~ 100 s) tail that pulsated with a period of ~ 8 s (Terrell et al. 1980). The total emitted energy during the initial peak and the decaying tail amounted to an astonishing $\sim 10^{44}$ erg.

An even more energetic flare was detected from SGR 1900+14 on August 27, 1998 by a multitude of space telescopes in the direction of a Galactic supernova remnant G42.8+0.6 (Hurley et al. 1999a), making it the second exceptionally energetic event detected in the past century from a recurrent gamma-ray source. The burst had properties

* E-mail: rsgill@phas.ubc.ca

† E-mail: hey1@phas.ubc.ca; Canada Research Chair

similar to that of the March 5 event, with a short (< 4 ms) rise time to the main peak that lasted for ~ 1 s and then decayed into a pulsating tail with a period identical to the rotation period of the NS of 5.16 s. The flare had a much harder energy spectrum compared to the March 5 event (Feroci et al. 1999), with peak luminosity in excess of $\sim 4 \times 10^{44}$ erg s^{-1} , assuming a distance of ~ 10 kpc to the source. The total energy unleashed in this outburst amounted to $\sim 10^{44}$ erg in hard X-rays and gamma-rays (Mazets et al. 1999).

Finally, on December 27, 2004 the most energetic outburst ever to be detected came from SGR 1806-20 (Hurley et al. 2005), a Galactic source that was found to have a possible association with a compact stellar cluster at a distance of ~ 15 kpc (Corbel & Eikenberry 2004). The initial spike had a much shorter rise time (≤ 1 ms) to the peak luminosity of $\sim 2 \times 10^{47}$ erg s^{-1} which persisted for a mere ~ 0.2 s. Like other giant flares, a hard X-ray tail, of duration ~ 380 s, followed the main spike pulsating at a period of 7.56 s. The total energies emitted during the initial spike and the harmonic tail are $\sim 4 \times 10^{46}$ erg and $\sim 10^{44}$ erg, respectively.

1.1 The Precursor

Hurley et al. (2005) reported the detection of a ~ 1 s long precursor that was observed 142 s before the main flare of December 27. A similar event, lasting a mere 0.05 s (Ibrahim et al. 2001), was observed only 0.4 s prior to the August 27 giant flare (Hurley et al. 1999a; Feroci et al. 2001), albeit at softer energies (15 – 50 keV, Mazets et al. 1999); a non detection at harder energies (40 – 700 keV) was reported in Feroci et al. (1999). Such a precursor was not detected at all for the March 5 flare for which the detectors at the time had no sensitivity below ~ 50 keV, which suggests that a softer precursor, if there indeed was one, may have gone unnoticed. Unlike the August 27 precursor, which was short and weak and for which no spectrum could be obtained (Ibrahim et al. 2001), the relatively longer lasting December 27 precursor had a thermal blackbody spectrum with $kT \approx 10.4$ keV (Boggs et al. 2007). In comparison to the common short SGR bursts, that typically last for ~ 0.1 s and have sharply peaked pulse morphologies, the December 27 precursor was not only longer in duration but also had a nearly flat light curve. Nevertheless, the burst packed an energy $\sim 3.8 \times 10^{41}$ erg which is comparable to that of the short SGR bursts. The possible causal connection of the precursors to the giant flares in both cases indicates that they may have acted as a final trigger (Hurley et al. 1999a; Boggs et al. 2007). A strong case for the causal connection of the precursor to the giant flare in both events can be established on statistical grounds. For example, SGR 1900+14 emitted a total of 50 bursts during its reactivation between May 26 and August 27, 1998 following a long dormant phase lasting almost 6 years (Hurley et al. 1999b). Here we are only interested in the burst history immediately prior to the Aug 27 event as this time period is indicative of the heightened activity that concluded with the giant flare. From these burst statistics, the rate of short bursts of typical duration ~ 0.1 s is $\sim 6 \times 10^{-6}$ s^{-1} , which then yields a null hypothesis probability of $\sim 2.4 \times 10^{-6}$ for the August 27 precursor. Additionally, we find a null hypothesis

probability of $\sim 8.6 \times 10^{-4}$ in the case of the December 27 precursor, assuming similar burst rates. Although the magnetar model (particularly the phenomenological models developed in Thompson & Duncan 1995, hereafter TD95, and Thompson & Duncan 2001, hereafter TD01), as we discuss below, offers plausible explanations for the occurrence of short bursts and giant flares, the connection between the precursor and the main flare has remained unknown. In the event the precursor indeed acted as a trigger to the main flare, it is of fundamental significance that the association between the two events is understood.

As magnetars, SGRs are endowed with extremely large magnetic fields with $B \sim 10^2 B_{\text{QED}}$, where $B_{\text{QED}} = 4.4 \times 10^{13}$ G is the quantum critical field, and all the energetic phenomena discussed above are ascribed to such high fields (TD95). In the the TD95 model, the short bursts result due to sudden cracking of the crust as it fails to withstand the building stresses caused by the motion of the magnetic footpoints. The slippage of the crust, as a result, injects Alfvén waves into the external magnetic field lines, that subsequently damp to higher wavenumbers, and ultimately dissipate into a trapped thermal pair plasma. Such a mechanism may not be invoked for the giant flares due to energy requirements. Alternatively, a large-scale interchange instability (Moffatt 1985), driven by the diffusion of the internal magnetic field, in combination with a magnetic reconnection event can power the giant flares. The plausibility of these mechanisms is well supported by the observed energetics of the bursts and the associated timescales. Nevertheless, a clear description of the reconnection process, which indubitably serves as one of the most efficient mechanisms to convert magnetic energy into heat and particle acceleration, has not been forthcoming. Furthermore, an alternative mechanism, motivated by the coronal heating problem in the solar case, can be formulated to give a reasonable explanation for the association of the precursor and the main flare.

In this paper, we propose two possible trigger mechanisms for the SGR giant flares - one internal and the other external to the NS. As we argue, either of the two trigger mechanisms can initiate the main hyperflare. In the following discussion, we calculate model parameters for the December 27 event, however, the analysis is similar for the other two events. We start with a discussion of the internal trigger in the next section, followed by that of the external trigger in Section 3. The discussion regarding some of the observed characteristics of the flares that our model can account for is presented in Section 4.

2 INTERNAL TRIGGER

In the magnetar model, the magnetic field in the interior of SGRs is considered to be strongly wound up which then generates a strong toroidal field component, possibly even larger than the poloidal component (TD01). The relative strengths of the poloidal and toroidal magnetic field components have been quantified by constructing relativistic models of NSs and testing the stability of axisymmetric fields by Lander & Jones (2009) and Ciolfi et al. (2009). Both studies arrive at the conclusion that the amplitude of the two field components may be comparable but the total mag-

netic energy is dominated by the poloidal component as the toroidal component is non-vanishing only in the interior, with $E_{B,\text{tor}}/E_B \leq 10$. However, in another study Braithwaite (2009) arrived at a somewhat different conclusion where he found a significant enhancement in the toroidal component to sustain a stable magnetic field configuration, with $0.20 \leq E_{B,\text{tor}}/E_B \leq 0.95$. In the interior, the twisted flux bundle, composed of several flux tubes, can be envisioned to stretch from one magnetic pole to the other along the symmetry axis of the dipole field that is external to the star. It has been shown by Parker (1983a,b) that any tightly wound flux bundle is unstable to dynamical nonequilibrium, and will dissipate its torsional energy as heat due to internal neutral point reconnection. Although Parker had provided such a solution to the long standing problem of coronal heating in the solar case, with a few exceptions, the same applies to the case of magnetars as the arguments are very general. In the case of the Sun, flux tubes are stochastically shuffled and wrapped around each other due to convective motions in the photosphere. Unlike in the Sun, where the flux tube footpoints are free to move in the photospheric layer, the footpoints are pinned to the rigid crust in NSs. Nevertheless, for exceptionally high magnetic fields ($B > 10^{15}$ G) the crust responds plastically (TD01), and any moderate footpoint motion can still occur. It is understood that this is only true to the point where the crustal stresses are below some threshold, which depends on the composition. Thus, as the imposed strain exceeds some critical value, the crust will yield abruptly (Horowitz & Kadau 2009), but may not fracture (Jones 2003).

Parker's solution is at best qualitative, however, it serves as a reasonably good starting point in the context of the present case. As we have noted earlier, the precursor may be causally connected to the main flare, and so can be argued to act as a trigger in the following manner. Immediately after the precursor the internal field evolves towards a new state of equilibrium. Since the crust has yielded to the built up stresses, and may deform plastically under magnetic pressure, some of the footpoints can now move liberally. Understandably, the turbulent dynamics, due to the high Reynolds number (Peralta et al. 2006), of the internal fluid in response to the burst translates into chaotic motion of the footpoints. As a result, the flux tubes are wrapped around each other in a random fashion. Current sheets then inevitably form leading to reconnection followed by violent relaxation of the twisted flux bundle. The heat flux resulting from the dissipation of the torsional energy of the flux bundle is given by Parker (1983a),

$$P = \left(\frac{B^2 v^2 \tau}{4\pi L} \right) \quad (1)$$

where B is the strength of the internal magnetic field, v is the footpoint displacement velocity, and L is the length scale of the flux tubes. Here τ is the timescale over which accumulation of energy by the random shuffling and wrapping of flux tubes occurs until some critical moment, after which neutral point reconnection becomes explosive. Having knowledge of the burst energetics, equation (1) can be solved for τ

$$\tau \sim 142 B_{15}^{-2} L_6^{-1} E_{46} T_{0.125}^{-1} \left(\frac{v}{8.4 \times 10^3 \text{ cm s}^{-1}} \right)^{-2} \text{ s} \quad (2)$$

where we have used the event of December 27 as an example, with internal field strength measured in units of 10^{15} G, flux tube length scales in 10^6 cm, the total energy of the flare in 10^{46} erg, and the timescale of the initial spike in 0.125 s (RHESSI PD time resolution). It is clear from equation (2) that the preflare quiescent time scales linearly with the total energy emitted in the initial spike but is inversely proportional to the internal magnetic field strength: $\tau \propto E_{\text{spike}} B_{\text{in}}^{-2}$. Following TD95, we have assumed that almost all of the energy of the flare was emitted in the initial transient phase during which the lightcurve rose to its maximum. Additionally, we find that the footpoints are displaced at a rate of few tens of meters per second, which is a reasonable estimate considering the fact that it is insignificant in comparison to the core Alfvén velocity $V_A \sim 10^7 \text{ cm s}^{-1}$.

A noteworthy point is that in regards to the burst energetics there is nothing special about the precursor when compared to the common SGR bursts, other than that it occurs at the most opportune time when the internal field undergoes a substantial reconfiguration. The mechanism outlined above is activated after every SGR burst after which significant footpoint motion ensues. However, whether the entanglement of flux tubes is sufficient to reach a critical state such that an explosive release of energy can occur depends on the evolution of the internal field configuration.

Alternatively, the twisted flux bundle can become unstable to a resistive instability, such as the tearing mode. The resistivity here is provided by the turbulent motion of the highly conductive fluid which is in a state of nonequilibrium immediately after the precursor. The growth time of the tearing mode instability is given by the geometric mean of the Alfvén time, say in the core, and the resistive timescale

$$\tau = (t_A t_R)^{1/2} \quad (3)$$

$$= \left(\frac{4\pi\sigma L^3}{V_A c^2} \right)^{1/2} \quad (4)$$

$$\sim 142 L_6^{3/2} \left(\frac{V_A}{10^7 \text{ cm s}^{-1}} \right)^{-1/2} \left(\frac{\sigma}{10^{13} \text{ s}^{-1}} \right)^{1/2} \text{ s} \quad (5)$$

where σ is not the electrical conductivity, but corresponds to the diffusivity of the turbulent fluid. In this case, the scaling for the preflare quiescent time becomes

$$\tau \propto E_{\text{spike}}^{1/2} B_{\text{in}}^{-3/2} \quad (6)$$

where we have assumed that the twisted flux bundle occupied the entire internal region of the NS.

3 EXTERNAL TRIGGER

The notion that the giant flares are a purely magnetospheric phenomena appears very promising and requires further development. A magnetospheric reconnection model has become the favourite of many for two main reasons. First, it can easily explain the millisecond rise times of the explosive giant flares in terms of the Alfvén time of the inner magnetosphere, which for exceptionally low values of the plasma beta parameter is very small; $\tau_A \sim R_*/c \sim 30\mu\text{s}$. Second, the SGR giant flares have much in common with the extensively studied solar flares, for which reconnection models

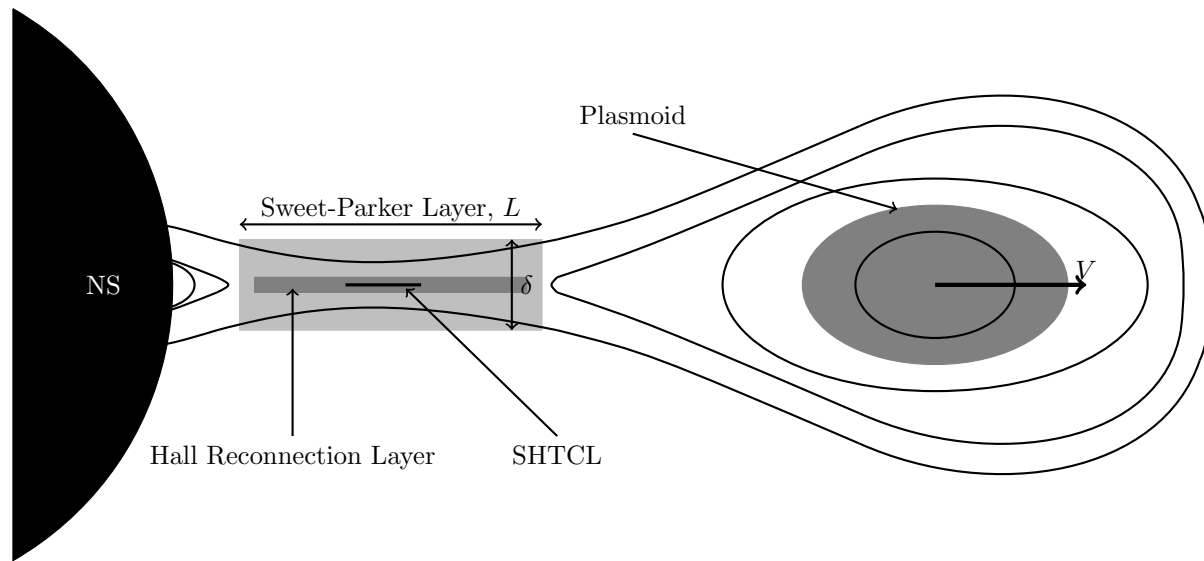


Figure 1. This figure displays the setup of the different reconnecting current layers. The macroscopic Sweet-Parker layer with length $L \sim 10^5$ cm and width $\delta \sim 0.01$ cm is the largest of the three. This layer is then thinned down vertically as strong magnetic flux is convected into the dissipation region. The Hall reconnection layer, represented by the dark gray region, develops when δ becomes comparable to the ion-inertial length d_i . The system makes a transition from the slow to the impulsive reconnection and powers the main flare. The tiny region embedded inside the Sweet-Parker layer is the super-hot turbulent current layer, which aids in creating sufficient anomalous resistivity to facilitate the formation of the Sweet-Parker layer. The strongly accelerated plasma downstream of the reconnection layer is trapped inside magnetic flux lines and forms a plasmoid moving at some speed V . This plasmoid is then finally ejected during the initial spike when the external field undergoes a sudden relaxation (After Lyutikov 2006).

explaining nonthermal particle creation, plasma bulk motions, and gas heating have been developed over the last few decades (Lyutikov 2002). The most powerful solar flares release an equally impressive amounts of energy $\sim 10^{32}$ erg, which is mainly divided into heating the plasma and radiation in multiple wavebands, for example γ -rays, X-rays, and radio. The impulsive rise in the soft X-ray emission to peak luminosity occurs over a timespan of few hundreds of seconds, which is then followed by a gradual decay lasting several hours (Priest & Forbes 2002). In the magnetar model, because of the shearing of the magnetic footpoints caused by the unwinding of the internal field, a twist can be injected into the external magnetic field (TD95,TD01). Depending on how the crust responds to the stresses, either plastically or rigidly, the gradual or sudden (in the event of a crustal fracture) transport of current from the interior creates a non-potential region in the magnetosphere where a reconnecting current layer can develop (Thompson et al. 2002; Mikic & Linker 1994). Lyutikov (2003, 2006) has explained the impulsive nature of the giant flares in terms of the tearing mode instability, which has a magnetospheric growth time of $\tau_{\text{tear}} \sim 10$ ms.

Impulsiveness of the underlying magnetic reconnection mechanism explaining the origin of giant flares is a primary requirement. The tearing mode instability is quite befitting in that regard; however, it has not been shown to bear any dependence on the precursor, which as we argue, triggered the main hyperflare. Hall reconnection, which is another impulsive reconnection mechanism, has been completely ignored on the basis that it is unable to operate in a mass symmetric electron-positron pair plasma. Nevertheless, a mild baryon contamination may be enough to render it operational. Therefore, what is needed here is the synergy of

two distinct mechanisms — a slow reconnection process, like the Sweet-Parker solution, that only dissipates magnetic energy at a much longer timescale (Sweet 1958; Parker 1957), and a fast process that is explosive, like Hall reconnection (Bhattacharjee et al. 1999). To put this in the context of the December 27 event, we envision that immediately after the precursor a macroscopic current layer developed as a result of the sheared field lines. Then began the slow dissipation of magnetic field energy by Sweet-Parker reconnection, which continued throughout the quiescent state that followed the precursor. Finally, the transition to Hall reconnection resulted in the explosive release of energy (see figure 1). We describe this process in more detail in the following section.

3.1 Transition from Resistive to Collisionless Reconnection by Current Sheet Thinning

The steady state reconnection process of Sweet and Parker is severely limited by its sensitivity to the size of the macroscopic dissipation region, such that the plasma inflow velocity is regulated by the aspect ratio of the current layer

$$v_i = \frac{\delta}{L} v_A \quad (7)$$

where δ is the width and L is the length of the dissipation region, with $\delta \ll L$ generally. The downstream plasma flow speed coincides with the Alfvén velocity, which in the magnetar case approaches the speed of light. The Sweet-Parker mechanism is a resistive reconnection process where the resistivity is either collisional or anomalous. It is understood that the electron-positron pair plasma pervading the inner magnetosphere is collisionless. Nevertheless, if enough ions are present in the dissipation region, as we show below,

then a source of anomalous resistivity can be established. We argue that the energy released during the precursor was enough to heat the crust to a point where a baryon layer was evaporated into the magnetosphere. TD95 provide an upper limit to the mass of the baryon layer ablated during a burst by comparing the thermal energy of the burst to that of the potential energy of the mass layer

$$\Delta M \sim \frac{E_{\text{th}} R_{\star}}{GM_{\star}} \quad (8)$$

$$\sim 10^{17} \left(\frac{E_{\text{th}}}{10^{38} \text{ erg}} \right) \left(\frac{R_{\star}}{10^6 \text{ cm}} \right) \left(\frac{M_{\star}}{1.4 M_{\odot}} \right) \text{ g} \quad (9)$$

where we have assumed a more conservative estimate of E_{th} . Then, assuming that ΔM amount of baryonic mass, in the form of protons, was injected into the magnetospheric volume of $\sim R_{\star}^3$ yielding a baryon number density of

$$n_b \sim 6 \times 10^{22} \left(\frac{E_{\text{th}}}{10^{38} \text{ erg}} \right) \left(\frac{R_{\star}}{10^6 \text{ cm}} \right)^{-2} \left(\frac{M_{\star}}{1.4 M_{\odot}} \right) \text{ cm}^{-3} \quad (10)$$

Even with the large amount of baryons, the magnetospheric plasma is still collisionless. The Spitzer resistivity for a quasi-neutral electron-ion plasma is only a function of the electron temperature $\propto T_e^{-3/2}$, which for electron temperatures as high as $\sim 10^8$ K yields a negligible resistivity.

3.1.1 Super-Hot Turbulent Current Layer

For plasma temperatures higher than $T > 3 \times 10^7$ K, the reconnecting current layer turns into a super-hot turbulent current layer (SHTCL), for which the theory has been well developed by and documented in (Somov 2006, pp. 129-151). The anomalous resistivity in the current layer arises due to wave-particle interactions, where the ions interact with field fluctuations in the waves. As a result, the resistivity and other transport coefficients of the plasma are altered. The electrons are the current carriers and participate mainly in the heat conductive cooling of the SHTCL. The current layer is assumed to have been penetrated by a relatively weak transverse magnetic field component (transverse to the electric field in the current layer), where $B_{\perp} \ll B_0$ with B_0 as the strength of the external dipole field. In the two temperature model, where the electrons and ions are allowed to have dissimilar temperatures, the effective anomalous resistivity is generally a combination of two terms. One resulting from the ion-acoustic turbulence and the other from the ion-cyclotron turbulence.

$$\eta_{\text{eff}} = \eta_{\text{ia}} + \eta_{\text{ic}} \quad (11)$$

In addition, each turbulent instability has two separate regimes – marginal and saturated. The former applies when the wave-particle interactions are described by quasilinear equations, and the latter becomes important in the case of strong electric fields when the nonlinear contributions can no longer be ignored (see for e.g. Somov 1992 pp. 115-217 for a detailed description). For an equal temperature plasma ($T_e \sim T_i$), the saturated ion-cyclotron turbulent instability makes the dominant contribution to the effective resistivity. Thus, we ignore any other terms corresponding to the ion-acoustic instability. The effective resistivity in the present case is given as (Somov 2006), depending on the dimensionless temperature parameter $\theta \equiv T_e/T_i$,

$$\eta_{\text{eff}} = \frac{2m_e^{1/2} \pi^{1/4}}{ec^{1/2} m_p^{1/4}} \left[\frac{(1 + \theta^{-1})^{1/2}}{N^{1/4}(\theta) U_k(\theta)} \right] \frac{(B_{\perp} E_0)^{1/2}}{B_0^{1/2} n_b^{3/4}} \quad (12)$$

where

$$N(\theta) = 1.75 + \frac{f(\theta)}{\sqrt{8(1 + \theta^{-1})^{3/2}}} \quad (13)$$

$$f(\theta) = \frac{1}{4} \left(\frac{m_p}{m_e} \right)^{1/2} \text{ for } 1 \leq \theta \leq 8.1 \quad (14)$$

$$U_k(\theta) \sim \mathcal{O}(1) \text{ for } \theta \sim 1 \quad (15)$$

$$E_0 = \alpha B_0 \quad (16)$$

$\alpha \equiv v_0/c$ is the effective reconnection rate determined by the inflow fluid velocity v_0 into the current layer, and the rest of the variables in equation (12) retain their usual meaning. Equation (16) conveys the frozen-in field condition. Next, we write the magnetic diffusivity of the plasma due to the effective anomalous resistivity

$$\eta_{\text{diff}} = \frac{\eta_{\text{eff}} c^2}{4\pi} \quad (17)$$

$$\simeq 6 \times 10^{23} (\alpha B_{\perp})^{1/2} n_0^{-3/4} \quad (18)$$

To calculate the inflow plasma velocity, we assume that the SHTCL is embedded in a macroscopic Sweet-Parker current layer. The primary role of the SHTCL is to provide enough resistivity in a collisionless plasma so that the magnetic field lines can diffuse through it and ultimately undergo reconnection. From equation (7) we know that for a Sweet-Parker current layer the inflow fluid velocity is regulated by the aspect ratio of the current layer. The outflow velocity is limited by the speed of light. By expressing the width of the Sweet-Parker current layer in terms of the magnetic diffusivity, we find that the inflow velocity has to be on the order of $v_0 \sim 10^3 \text{ cm s}^{-1}$ (so that $\alpha \ll 1$), with the width of the layer given as

$$\delta \sim \sqrt{\frac{\eta_{\text{diff}} L}{c}} \quad (19)$$

$$\sim 0.01 \text{ cm} \left(\frac{v_0}{10^3 \text{ cm s}^{-1}} \right)^{1/4} \left(\frac{B_{\perp}}{10^{11} \text{ G}} \right)^{1/4} \times \left(\frac{n_b}{6 \times 10^{22} \text{ cm}^{-3}} \right)^{-3/8} \left(\frac{L}{10^5 \text{ cm}} \right)^{1/2} \quad (20)$$

where the transverse magnetic field is $B_{\perp} \sim 10^{-3} B_0$, and L is the length of the current layer. The size of the SHTCL can now be obtained from the following

$$a = \frac{c}{e} \sqrt{\frac{m_e}{2\pi n_b}} \left[\sqrt{\frac{1 + \theta^{-1}}{N(\theta)}} \frac{1}{U_k(\theta)} \right] \quad (21)$$

$$\sim 2.5 \times 10^{-6} \left(\frac{n_b}{6 \times 10^{22} \text{ cm}^{-3}} \right)^{-1/2} \text{ cm} \quad (22)$$

$$b = \frac{B_0}{h_0} \sqrt{\frac{2v_0}{B_{\perp}}} \left[\frac{\pi m_p n_b}{N(\theta)} \right]^{1/4} \quad (23)$$

$$\sim 80 \text{ cm} \left(\frac{R_{\star}}{10^6 \text{ cm}} \right) \left(\frac{v_0}{10^3 \text{ cm s}^{-1}} \right)^{1/2} \times \left(\frac{B_{\perp}}{10^{11} \text{ G}} \right)^{-1/2} \left(\frac{n_b}{6 \times 10^{22} \text{ cm}^{-3}} \right)^{1/4} \quad (24)$$

where a and b are, respectively, the half-width and the half-length of the SHTCL, and $h_0 \sim B_0/R_{\star}$ is the magnetic field gradient in the vicinity of the current layer.

3.1.2 Current Sheet Thinning

The main flare is triggered when the transition is made from the steady state, slow reconnection process to an impulsive one. In the present case, Sweet-Parker reconnection makes a transition to Hall reconnection when the width of the current layer δ drops below the ion-inertial length d_i , where

$$d_i = \frac{c}{\omega_{p,i}} = \frac{c}{e} \sqrt{\frac{m_p}{4\pi n_b}} \quad (25)$$

$$\sim 10^{-4} \left(\frac{n_b}{6 \times 10^{22} \text{ cm}^{-3}} \right)^{-1/2} \text{ cm} \quad (26)$$

and $\omega_{p,i}$ is the non-relativistic ion plasma frequency. Cassak et al. (2005) show that for a given set of plasma parameters, the solution is bistable such that the slow Sweet-Parker solution can operate over long timescales, during which the system can accumulate energy, while the faster Hall solution starts to dominate as the resistivity is reduced below some critical value. Lowering the resistivity would naturally reduce the width of the current layer to the point where the system can access the Hall mechanism. Alternatively, as Cassak et al. (2006) argue, the same result can be achieved by thinning down the current layer by convecting in stronger magnetic fields into the dissipation region during Sweet-Parker reconnection. The critical field strength needed to thin the current layer is

$$B_c \sim \sqrt{4\pi m_p n_b} \left(\frac{\eta_{\text{diff}}}{d_i^2} L \right) \quad (27)$$

$$\begin{aligned} &\sim 4 \times 10^{14} \text{ G} \left(\frac{n_b}{6 \times 10^{22} \text{ cm}^{-3}} \right)^{3/4} \\ &\times \left(\frac{v_0}{10^3 \text{ cm s}^{-1}} \right)^{1/2} \left(\frac{B_{\perp}}{10^{11} \text{ G}} \right)^{1/2} \left(\frac{L}{10^5 \text{ cm}} \right) \end{aligned} \quad (28)$$

Due to flux pile up outside the current layer, it can be argued that the system is able to achieve such high field strengths. The timescale for thinning down the current sheet until its width is comparable to the ion-inertial length is given as

$$\tau_{\text{thin}} \sim 2W_s \sqrt{\frac{L}{\eta_{\text{diff}} c} \left(\frac{B_c}{B_0} \right)} \quad (29)$$

$$\begin{aligned} &\sim 130 \text{ s} \left(\frac{W_s}{10^5 \text{ cm}} \right) \left(\frac{L}{10^5 \text{ cm}} \right) \left(\frac{B_0}{10^{14} \text{ G}} \right)^{-1/2} \\ &\times \left(\frac{n_b}{6 \times 10^{22} \text{ cm}^{-3}} \right)^{3/4} \end{aligned} \quad (30)$$

where W_s is the magnetic shear length, that is the length scale over which the field lines are severely sheared. What we find here is that the thinning down time τ_{thin} of the current layer from the Sweet-Parker width to the ion-inertial length, where Hall reconnection dominates, is on the order of the preflare quiescent time of ~ 142 s for the December 27 event. The scaling relation of the thinning down time in terms of the initial spike energy and the external magnetic field strength can be deduced to be the following

$$\tau_{\text{thin}} \propto E_{\text{spike}}^{2/3} B_0^{-11/6} \quad (31)$$

Again, we emphasize here that this same mechanism may operate after every SGR burst which is energetic enough to inject the requisite baryon number density, as calculated in equation (10), to facilitate the development of a Sweet-Parker current layer. However, this mechanism will fail if the twist injected into the magnetosphere by the unwinding

of the internal field is not sufficient to create a tangential discontinuity at the first place. In that instance no current sheet will form.

3.1.3 Giant flare Submillisecond Rise Times

In Hall reconnection, a multiscale dissipation region develops with characteristic spatial scales on the order of the ion and electron inertial lengths (Shay et al. 2001). Within a distance d_i of the neutral X-line, the ions decouple from the electrons and are accelerated away at Alfvénic speeds in the direction perpendicular to that of the inflow. The electrons continue their motion towards the neutral line as they are frozen-in, and only decouple from the magnetic field when they are a distance d_e , the electron-inertial length, away from the neutral line. Within the ion-inertial region, the dynamics of the electrons are significantly influenced by the nonlinear whistler waves. Subsequently, the electrons too are accelerated away in an outflowing jet at Alfvénic speeds. The timescale associated to Hall reconnection then is in good accord with the rise times of giant flares (Schwartz et al. 2005), that is

$$\tau_{\text{Hall}} \sim \frac{R_*}{0.1c} \sim 0.3 \text{ ms} \quad (32)$$

4 DISCUSSION

In this paper, we present an internal and an external trigger mechanism for the SGR giant flares, where we strongly emphasize the causal connection of the precursor to the main flare. The quiescent state that follows the precursor has been argued, in our model, to be the time required for the particular instabilities to develop, along with the accumulation of energy just before the flare. The internal mechanism is based on the hypothesis that poloidal field component in the interior of the NS is strongly wound up. The solution is motivated by Parker's reasoning that such a twisted field would inevitably develop tangential discontinuities and dissipate its torsional energy as heat. The timescale for the accumulation of energy that is to be released in the main flare is on the order of the duration of the preflare quiescent state.

The external trigger mechanism makes use of the fact that a Sweet-Parker reconnection layer may develop between significantly sheared field lines if a source of resistivity is established. Such a source may be embedded inside the macroscopic Sweet-Parker layer in the form of a super-hot turbulent current layer. To make the reconnection process impulsive, we invoke the non-steady Hall reconnection which is switched on as the width of the Sweet-Parker layer is thinned down to the ion-inertial length. Again, the timescale over which the layer is thinned down roughly coincides with that of the preflare quiescent state duration.

We have shown detailed calculations of the timescales for the December 27 event in particular. However, a similar analysis can also be carried out for the August 27 event. For the internal mechanism, we find the timescale to be comparable to the observed preflare quiescent time with $\tau \sim 0.4 B_{15}^{-2} L_6^{-1} E_{44} T_1^{-1} \left(\frac{v}{5.6 \times 10^4 \text{ cm s}^{-1}} \right)^{-2}$ s, where we have assumed the same internal magnetic field strength and

length of flux tubes. For the external mechanism, assuming $\Delta M \sim 10^{15}$ g, since the precursor was short and weak, $W_s \sim 2 \times 10^4$, and $L \sim 5 \times 10^4$, we find $\tau_{\text{thin}} \sim 0.4$ s, $\delta \sim 0.04$ cm, $a \sim 2.5 \times 10^{-5}$ cm, $b \sim 25$ cm, and $d_s \sim 10^{-3}$ cm.

A significant nonthermal component, with an average power-law index of $\Gamma \sim 2$ as in $E^{-\Gamma}$, was observed during the decaying phase of the flare in both the August 27 and December 27 events (Feroci et al. 1999; Boggs et al. 2007). In the magnetar model, the nonthermal emission originates much farther out from the star, almost at the light cylinder (TD01). At this distance, inverse Compton cooling by X-ray photons has been invoked to explain the nonthermal spectrum. Nonthermal particle generation is one of readily identified features of magnetic reconnection, especially in the case of Hall reconnection where outflow velocities approach the Alfvén speed of the medium. Such acceleration of high energy particles due to meandering-like orbits in the presence of strong electric fields has also been seen in particle-in-cell simulations (Zenitani & Hoshino 2001). Therefore, the Hall reconnection process that gives rise to the main flare can easily explain the origin of nonthermal particles.

Israel et al. (2005) and Strohmayer & Watts (2005) reported the detection of quasi-periodic oscillations (QPOs) in the burst spectra of the December 27 and August 27 events, respectively. QPOs in the December 27 event were detected at 92.5 Hz, and 18 and 30 Hz at, respectively, 170 s and $\sim 200 - 300$ s after the initial spike. Watts & Strohmayer (2006) confirmed the detection of the first two QPOs and reported the presence of two additional QPOs at 26 and 626.5 Hz. Similarly, in the August 27 event, QPOs at 84 Hz, 53.5 Hz, 155.1 Hz, and 28 Hz (with lower significance) were detected at about a minute after the onset of the flare. Torsional oscillation of the NS crust appeared to be the natural explanation for the QPOs. However, Levin (2006) argues that purely crustal oscillations rapidly lose their energy to an Alfvén continuum in the core by resonant absorption. He demonstrates that steady low frequency oscillations can be associated with MHD continuum turning points in the core (Levin 2007), while others have reproduced the QPOs in toy models governed by global MHD-elastic modes of the NS (Glampedakis et al. 2006; Sotani et al. 2007). Both trigger mechanisms presented in this paper can be linked to the initiation of such an oscillatory behavior, whether in the core or as a global mode of the star, by the realization that during the giant flare the global magnetic field of the star undergoes sudden magnetic relaxation (TD95). In the internal trigger, the sudden loss of helicity can be argued to be sufficient to launch Alfvén waves in the interior.

On the other hand, although the external trigger, is not directly tied to the crust, however, a sudden relaxation of the internal toroidal field in the sense of the Flowers & Ruderman (1977) instability can be realized. The loss of magnetic energy in the form of a plasmoid, which has been known to form during an eruptive flare (Magara & Shibata 1997), serves to relax both the sheared external dipole field and the twisted internal toroidal field. Since both fields thread through the entire star, a sudden relaxation during the initial spike can easily excite global elastic modes in the NS. The ejection of a plasmoid also naturally explains the origin of the radio afterglow observed for both the August 27 and the December 27 events (Frail et al.

1999; Gaensler et al. 2005; also see Lyutikov 2006 for afterglow geometry and parameters).

In our calculations, we have shown how the preflare quiescent time scales with the total energy released in the initial spike. In the internal trigger mechanism, we find that Parker’s solution yields a linear dependence. Although, as we have remarked earlier, this mechanism is simple and elegant but based on qualitative arguments. Nevertheless, it does reproduce the observed result, that is the longer the preflare quiescent time the energetic the flare, if the internal magnetic field strengths for both NSs are assumed to be similar: $\tau_{\text{Aug}}/\tau_{\text{Dec}} \sim E_{\text{Aug}}/E_{\text{Dec}}$. On the other hand, for the scaling to reconcile with observations in the case of the tearing mode instability and the external trigger, either $E_{\text{Aug}}/E_{\text{Dec}} \ll 10^{-3}$ or $B_{1900+14}/B_{1806-20} \gg 10^{-1}$. Based on the measured P and \dot{P} values for SGR 1900+14 and SGR 1806-20, which suggest that $B_{1806-20} \sim 3B_{1900+14}$, and with the revised distance estimate of $D \sim 12 - 15$ kpc for SGR 1900+14 (Vrba et al. 2000), neither condition may be satisfied. However, one should not ignore the fact that the external mechanism also depends on the size of the current layer and the field line shearing lengthscale. Therefore, the scaling relation may not be as simple as that argued in equation (31). In any case, with only two events it is premature to observe any trends regarding the preflare quiescent times and the burst energies. Future giant flares from SGRs will certainly improve our understanding of such correlations.

ACKNOWLEDGEMENTS

We would like to thank the anonymous reviewer for his help in improving the quality of this paper. R.G. is supported by NSERC CGS-D3 scholarship. The Natural Sciences and Engineering Research Council of Canada, Canadian Foundation for Innovation and the British Columbia Knowledge Development Fund supported this work. Correspondence and requests for materials should be addressed to J.S.H. (hey1@phas.ubc.ca). This research has made use of NASA’s Astrophysics Data System Bibliographic Services.

REFERENCES

- Bhattacharjee A., Ma Z. W., Wang X., 1999, *J. Geophys. Res.*, 104, 14543
- Boggs S. E., Zoglauer A., Bellm E., Hurley K., Lin R. P., Smith D. M., Wigger C., Hajdas W., 2007, *ApJ*, 661, 458
- Braithwaite J., 2009, *MNRAS*, 397, 763
- Cassak P. A., Drake J. F., Shay M. A., 2006, *ApJL*, 644, L145
- Cassak P. A., Shay M. A., Drake J. F., 2005, *Physical Review Letters*, 95, 235002
- Cioffi R., Ferrari V., Gualtieri L., Pons J. A., 2009, *MNRAS*, 397, 913
- Corbel S., Eikenberry S. S., 2004, *AA*, 419, 191
- Feroci M., Frontera F., Costa E., Amati L., Tavani M., Rapisarda M., Orlandini M., 1999, *ApJL*, 515, L9
- Feroci M., Hurley K., Duncan R. C., Thompson C., 2001, *ApJ*, 549, 1021
- Flowers E., Ruderman M. A., 1977, *ApJ*, 215, 302

- Frail D. A., Kulkarni S. R., Bloom J. S., 1999, *Nature*, 398, 127
- Gaensler B. M., Kouveliotou C., Gelfand J. D., Taylor G. B., Eichler D., Wijers R. A. M. J., Granot J., Ramirez-Ruiz E., Lyubarsky Y. E., Hunstead R. W., Campbell-Wilson D., van der Horst A. J., McLaughlin M. A., Fender R. P., Garrett M. A., 2005, *Nature*, 434, 1104
- Glampedakis K., Samuelsson L., Andersson N., 2006, *MNRAS*, 371, L74
- Helfand D. J., Long K. S., 1979, *Nature*, 282, 589
- Horowitz C. J., Kadau K., 2009, *Phys. Rev. Lett.*, 102, 191102
- Hurley K., Boggs S. E., Smith D. M., Duncan R. C., Lin R., Zoglauer A., Krucker S., Hurford G., Hudson H., Wigger C., Hajdas W., Thompson C., Mitrofanov I., Sanin A., Boynton W., Fellows C., von Kienlin A., Lichti G., Rau A., 2005, *Nature*, 434, 1098
- Hurley K., Cline T., Mazets E., Barthelmy S., Butterworth P., Marshall F., Palmer D., Aptekar R., Golenetskii S., Il'Inskii V., Frederiks D., McTiernan J., Gold R., Trombka J., 1999, *Nature*, 397, 41
- Hurley K., Kouveliotou C., Woods P., Cline T., Butterworth P., Mazets E., Golenetskii S., Frederiks D., 1999, *ApJL*, 510, L107
- Ibrahim A. I., Strohmayer T. E., Woods P. M., Kouveliotou C., Thompson C., Duncan R. C., Dieters S., Swank J. H., van Paradijs J., Finger M., 2001, *ApJ*, 558, 237
- Israel G. L., Belloni T., Stella L., Rephaeli Y., Gruber D. E., Casella P., Dall'Osso S., Rea N., Persic M., Rothschild R. E., 2005, *ApJL*, 628, L53
- Jones P. B., 2003, *ApJ*, 595, 342
- Kaneko Y., Göğüş E., Kouveliotou C., Granot J., Ramirez-Ruiz E., van der Horst A. J., Watts A. L., Finger M. H., Gehrels N., Pe'er A., van der Klis M., von Kienlin A., Wachter S., Wilson-Hodge C. A., Woods P. M., 2010, *ApJ*, 710, 1335
- Kumar H. S., Ibrahim A. I., Safi-Harb S., 2010, *ArXiv e-prints*
- Lander S. K., Jones D. I., 2009, *MNRAS*, 395, 2162
- Levin Y., 2006, *MNRAS*, 368, L35
- Levin Y., 2007, *MNRAS*, 377, 159
- Lyutikov M., 2002, *ApJL*, 580, L65
- Lyutikov M., 2003, *MNRAS*, 346, 540
- Lyutikov M., 2006, *MNRAS*, 367, 1594
- Magara T., Shibata K., 1997, *Advances in Space Research*, 19, 1903
- Mazets E. P., Golenskii S. V., Ilinskii V. N., Aptekar R. L., Guryan I. A., 1979, *Nature*, 282, 587
- Mazets E. P., Cline T. L., Aptekar' R. L., Butterworth P. S., Frederiks D. D., Golenetskii S. V., Il'Inskii V. N., Pal'Shin V. D., 1999, *Astronomy Letters*, 25, 635
- Mereghetti S., 2008, *Astron. Astrophys. Rev.*, 15, 225
- Mikic Z., Linker J. A., 1994, *ApJ*, 430, 898
- Moffatt H. K., 1985, *Journal of Fluid Mechanics*, 159, 359
- Parker E. N., 1957, *J. Geophys. Res.*, 62, 509
- Parker E. N., 1983a, *ApJ*, 264, 642
- Parker E. N., 1983b, *ApJ*, 264, 635
- Peralta C., Melatos A., Giacobello M., Ooi A., 2006, *ApJ*, 651, 1079
- Priest E. R., Forbes T. G., 2002, *A&ARv*, 10, 313
- Schwartz S. J., Zane S., Wilson R. J., Pijpers F. P., Moore D. R., Kataria D. O., Horbury T. S., Fazakerley A. N., Cargill P. J., 2005, *ApJL*, 627, L129
- Shay M. A., Drake J. F., Rogers B. N., Denton R. E., 2001, *J. Geophys. Res.*, 106, 3759
- Somov B. V., ed. 1992, *Physical processes in solar flares*. Vol. 172 of *Astrophysics and Space Science Library*
- Somov B. V., ed. 2006, *Plasma astrophysics, part II : reconnection and flares*. Vol. 341 of *Astrophysics and Space Science Library*
- Sotani H., Kokkotas K. D., Stergioulas N., 2007, *MNRAS*, 375, 261
- Strohmayer T. E., Watts A. L., 2005, *ApJL*, 632, L111
- Sweet P. A., 1958, in B. Lehnert ed., *Electromagnetic Phenomena in Cosmical Physics* Vol. 6 of *IAU Symposium, The Neutral Point Theory of Solar Flares*. pp 123+
- Terrell J., Evans W. D., Klebesadel R. W., Laros J. G., 1980, *Nature*, 285, 383
- Thompson C., Duncan R. C., 1995, *MNRAS*, 275, 255
- Thompson C., Duncan R. C., 2001, *ApJ*, 561, 980
- Thompson C., Lyutikov M., Kulkarni S. R., 2002, *ApJ*, 574, 332
- van der Horst A. J., Connaughton V., Kouveliotou C., Göğüş E., Kaneko Y., Wachter S., Briggs M. S., Granot J., Ramirez-Ruiz E., Woods P. M., Aptekar R. L., Barthelmy S. D., Cummings J. R., Finger M. H., Frederiks D. D., Gehrels N., Gelino C. R., Gelino D. M., Golenetskii S., Hurley K., Krimm H. A., Mazets E. P., McEnery J. E., Meegan C. A., Oleynik P. P., Palmer D. M., Pal'shin V. D., Pe'er A., Svinkin D., Ulanov M. V., van der Klis M., von Kienlin A., Watts A. L., Wilson-Hodge C. A., 2010, *ApJ, Letters*, 711, L1
- Vrba F. J., Henden A. A., Luginbuhl C. B., Guetter H. H., Hartmann D. H., Klose S., 2000, *ApJL*, 533, L17
- Watts A. L., Strohmayer T. E., 2006, *ApJL*, 637, L117
- Woods P. M., Thompson C., 2006, *Soft gamma repeaters and anomalous X-ray pulsars: magnetar candidates*. pp 547-586
- Zenitani S., Hoshino M., 2001, *ApJL*, 562, L63